Original paper

B-ultrasound or CT-guided 3D-printing individualized non-coplanar template brachytherapy for the treatment of locally uncontrolled recurrent head and neck squamous cell carcinoma

Pengbing Han, Fengju Li, Yanping Zhang, Liying Gao, Guiqiong Zhang, Qing Guo, Yuxia Zhu, Qun Su

Department of Radiotherapy, Gansu Provincial Cancer Hospital, Lanzhou, China

Adv Dermatol Allergol 2024; XLI (1): 41–48
DOI: https://doi.org/10.5114/ada.2024.136252

Abstract

Introduction: It is worth to explore a more effective treatment method to minimize the damage for patients during the treatment process.

Aim: To explore the method, feasibility and efficacy of B-ultrasound or computed tomography (CT)-guided 3D printing individualized non-coplanar template brachytherapy in the treatment of locally uncontrolled recurrent head and neck squamous cell carcinoma.

Material and methods: Ten patients with locally uncontrolled recurrent head and neck squamous cell carcinoma who were treated in our department from August 2021 to February 2023 were collected and treated by 3D printing individualized non-coplanar template brachytherapy under the guidance of B-ultrasound or CT, using the 192Ir high-dose rate afterloading treatment machine of NUCLETRON Technologies GmbH. The radiation source was 192Ir, with a diameter of 0.5 mm, a length of 3.5 mm, a total dose of 10–24 Gy, 5–8 Gy/time, once a week.

Results: According to the efficacy evaluation criteria, CT scan was performed after 1-6 months, followed up for 24 months, including CR 40% (4/10), PR 50% (5/10), NC 10% (5/10), PD 0 (0). The total effective rate of CR + PR was 90% (9/10), the 6-month local control rate was 90%, the 12-month local control rate was 80%, the 18-month local control rate was 70%, and the 24-month local control rate was 70%. The overall survival rate at 24 months was 100%.

Conclusions: Safe and effective interpolation is used to guide the 3D printing of a single non-coplanar template with B-ultrasound or CT in the radiotherapy of local and uncontrolled recurrent head and neck squamous cell carcinoma. According to the guidance of B-ultrasound or CT, the 3D printing individualized non-coplanar template has an obvious healing effect especially in the brachytherapy, and can also protect the functional organs well, with less side effects and fewer complications. Therefore, this method is the most effective for the treatment of locally uncontrolled recurrent head and neck squamous cell carcinoma.

Key words: 3D printing, close inter-tissue transplantation, local uncontrolled recurrence, squamous cell carcinoma of the head and neck.

Introduction

Radiotherapy stands as a crucial and efficacious method for treating tumors. According to the World Health Organization statistics, approximately 50% to 70% of tumor patients require radiotherapy [1, 2]. An experimental study reveals that head and neck squamous cell carcinoma ranks among the most prevalent malignant tumors. Head and neck squamous cell carcinomas (HNSCCs) originate from the mucosal epithelium in the oral cavity, pharynx, and larynx, representing the most prevalent malignancies in the head and neck region. The prevalence of HNSCC exhibits variation across countries and regions, typically associated with exposure to carcinogens derived from tobacco, excessive alcohol consumption, or both. Notably, tumors arising in the oropharynx are increasingly linked to past infections with oncogenic strains of human papillomavirus (HPV), primarily HPV-16, and to a lesser extent, HPV-18, along with other strains [3–5]. No screening method has demonstrated effectiveness, and a thorough physical examination remains the

Address for correspondence: Qun Su, Department of Radiotherapy, Gansu Provincial Cancer Hospital, Lanzhou 730050, China, e-mail: puyongzhang9273185@163.com
Received: 25.11.2023, **accepted:** 5.01.2024, **online publication:** 28.02.2024.

primary strategy for early detection. While some oral pre-malignant lesions (OPLs), such as leukoplakia (white patches) or erythroplakia (red patches), progress to invasive cancer, a significant number of patients present with advanced-stage HNSCC without a prior clinical history of pre-malignancy. Treatment for oral cavity HNSCC typically involves surgical resection, followed by adjuvant radiation or chemotherapy in conjunction with radiation, commonly referred to as chemoradiation or chemoradiotherapy (CRT), depending on the disease stage. CRT has been the primary therapeutic approach for addressing cancers arising in the pharynx or larynx [6].

Treatment options typically include surgery, standalone radiotherapy, or concurrent radiotherapy and chemotherapy. Patients often present at a locally advanced stage during treatment, resulting in a relatively poor prognosis with frequent occurrences of local uncontrolled growth and recurrence [7]. Currently, effective treatment modalities for these patients are lacking. Simple secondary surgeries, external irradiation, and chemotherapy often yield significant side effects, numerous complications, and limited efficacy [8]. Both local control and survival rates fall short of the desired benchmarks. Clinicians face the challenge of determining a treatment method that combines substantial efficacy with minimal side effects [9].

Aim

This study presents findings from the analysis of 10 patients with locally uncontrolled recurrent head and neck squamous cell carcinoma treated in our department between August 2021 and February 2023. Utilizing the hyperfractionation method guided by B-ultrasound or computed tomography (CT), take treatment of recurrent locally advanced head and neck tumors [10].

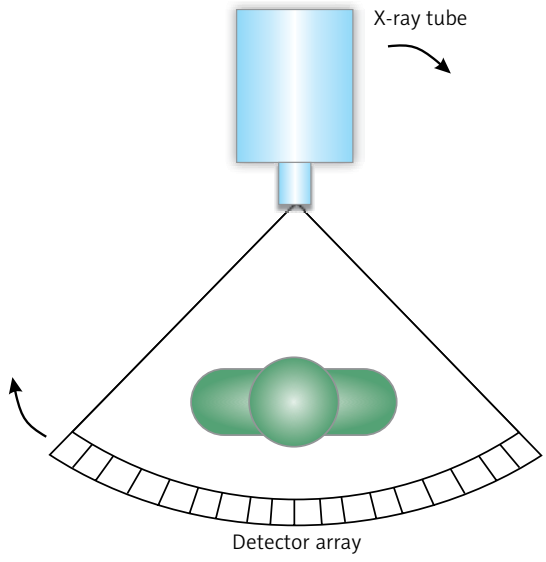

Figure 1. CT imaging principle

Material and methods

Preparation of a new type of ferric oxide nano developer

Principle of CT imaging and demand for developer

The famous German physicist Roentgen discovered an unknown ray in an experiment. Through research, it was learned that this ray can penetrate any opaque object (including bones and muscles) so as to make the fluorescent screen display images. This unknown ray is defined as X-ray [11]. The first X-ray transmission in history was found in the film of the handheld image laboratory, which is of great significance for further X-ray research. After X-ray was detected, it was rapidly applied to medical X-ray head-up imaging and other fields [12]. The emergence of CT technology has brought good news to the fields of medicine, food, materials, industry and aerospace. CT imaging is mainly used to capture the objects found from different angles by X-ray, obtain the measured data from a specific angle, and then digitize the projection data. It can be known through the restoration algorithm and the image displayed on the computer [13]. CT imaging can obtain the structural information about the actual object. This technology has enriched people's horizons to a certain extent and modified the content of object structure information [14]. Now the obstacles of traditional X-ray imaging have been overcome, and the actual value of X-ray has also been better reflected. In modern medicine, X-ray computed tomography is a simple imaging method. As a non-invasive imaging method, it is widely used in medical research and clinical practice. CT is characterized by 3D image reconstruction and target tissue segmentation [15]. The use of high-resolution CT system can perform harmless 3D imaging of various tissues and organs, including the gastrointestinal tract, cardiovascular system, kidney, liver, lung, bone, cartilage and tumor tissue [16, 17]. The four components of CT are: X-ray tube (used to generate X-ray), detector (used to obtain information), information program conversion and image display. As shown in Figure 1, the detector is located directly opposite the radioactive source, the person stands in the middle, and the X-ray source rotates around the object to obtain the image effect of CT. Many CT scanners used in the clinic have another layout, that is, sometimes the object rotates around its own axis. This clinical scanner is usually used for live imaging. Generally, X-ray scanning rotates around the object at a small angle of 360°. At the same time, this will also produce a series of attenuation layers. The 3D image of the scanned object can be obtained through arithmetic processing. The X-ray beam absorbs or deflects the tissue and contrast agent as it passes through the patient's body.

In order to increase the X-ray attenuation of biological tissue, we often introduce elements with high atoms into the contrast agent. The best choice for CT imaging is iodine. The combination of sodium iodide and lithium

iodide is the earliest contrast agent. However, they contain toxicity and are not suitable for clinical use. Therefore, covalently bound iodine is the best choice for designing contrast agents. At present, most of the iodine contrast agents used in clinical use are small molecular iodine contrast agents sold on the market, but they are easy to remove by the kidney and stay in the body for a short time. In recent years, in order to overcome the shortcomings of small molecular iodine contrast agents, nanoparticles containing iodine have emerged, mainly liposomes, nano-immunity and polymer iodine contrast agents. In this paper, Fe3O4 is combined with iodine to form new ferric oxide nanoparticles, which can be used as a contrast agent.

Preparation principle of developer

Magnetic nanomaterials can be used as CT contrast agents in the clinic. Magnetic materials commonly used as contrast agents include paramagnetic (e.g., gadolinium complexes) and nanoparticles with superparamagnetic properties (e.g., iron oxide). Compared with gadolinium contrast agents with toxicity problems, ferric oxide nanoparticles have stable properties and can be further modified and controlled as contrast agents. For a long time, the synthesis of Fe_3O_4 nanoparticles with good performance has been the most challenging in this technology. It is mainly hoped that it can synthesize nanoparticles with proper size, narrow particle size distribution, good purity and high crystallinity. These characteristics are essential for achieving good drug metabolism (PK) and drug efficacy (PD) of nanoparticles. The chemical surface structure of nanoparticles determines their PK/PD properties, while the phase purity and high crystallinity affect the contrast enhancement effect of imaging. Many effective synthesis methods have been used to produce high-quality Fe_3O_4 nanoparticles. Fe_3O_4 nanoparticles have stability, permeability and biocompatibility in terms of size and shape control.

The magnetism of an object is related to temperature and quantity. When the size of ferromagnet or ferrous magnet is reduced to a certain critical value, there is no permanent magnetic moment in the absence of the external magnetic field, but it can also respond in the presence of the external magnetic field, which is a superparamagnetic material. Superparamagnetic materials are widely used in many traditional fields, especially in biomedicine and related fields.

Preparation of a new type of ferric oxide nanometer developer

First, one should prepare 25 ml mixture (including $FeCl_2 \cdot 4\ H_2O$ (1 M), $FeCl_3 \cdot 6\ H_2O$ (0.5 M) and 0.4 M dilute hydrochloric acid), and remove nitrogen from the air by stirring; then one should prepare 250 ml of sodium hydroxide (NaOH), transfer it to a three-necked round bottom flask for further operation, heat it to 80°C, add 25 ml of prepared mixture into the NaOH solution, and then continue stirring for 2 h; after this reaction, one should let it cool naturally, collect the black residue, neutralize it with NaOH dilute hydrochloric acid, and finally separate and wash it 5 times to obtain stable Fe_3O_4 nanoparticles.

In PBS buffer solution (containing 0.5 M NaCl), one should combine 1 mg PGA or PLL with pH 7.4 to make 1 mg/ml PGA solution and PLL solution. After 20 min of adsorption, the solution should be centrifuged at 8000 rpm for 10 min, washed with water 3 times, and washed again in water to make solution A.

Then one should add 0.05, 0.1, 0.2, 0.5, 1 µl/ml (solvent: ethanol : water V : V = 1 : 9) iodized oil solution, the iodine (I) concentration after conversion of a, b, c, d and e is 24, 48, 96, 240 and 480 respectively µg/ml. Then one should take 5 parts of solution A and put them into a 2 ml centrifuge tube. One should add 1ml of solution into 5 centrifuge tubes and disperse them evenly in A, B, C, D and E for 3 h, centrifuge to excite the supernatant. After washing twice in water, one should disperse it in 1 ml of water, which can also obtain a new type of nanomaterial carrying iodinated oil.

Performance test of a new type of ferric oxide nano developer

Iodized oil is the main imaging technique. It has little damage to the human body and has a certain therapeutic effect. Iodine oil materials are insoluble in water and soluble in ethanol. When iodine oil is dissolved in ethanol/water mixed solution (the volume ratio of ethanol to water is 1 : 9), lotion is formed. During the process, Iodine oil is added to the solution. Iodine oil in lotion diffuses rapidly due to hydrophilicity and adheres to the propyl part of the aminopropyl group. The results are shown in Figure 2.

The absorption, distribution, metabolism, excretion and toxicity of iron tetroxide nanoparticles depend on their physical and chemical properties, such as density, size, surface charge, properties of surface chemical groups and redox activity. From the perspective of toxicity, the trace metal ele-

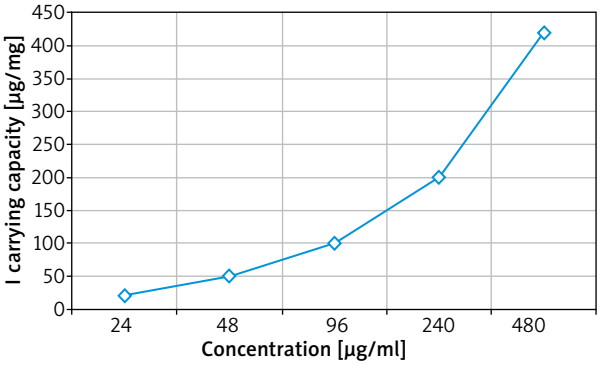

Figure 2. The carrier capacity of iodinated oil with different initial concentrations in new nanomaterials

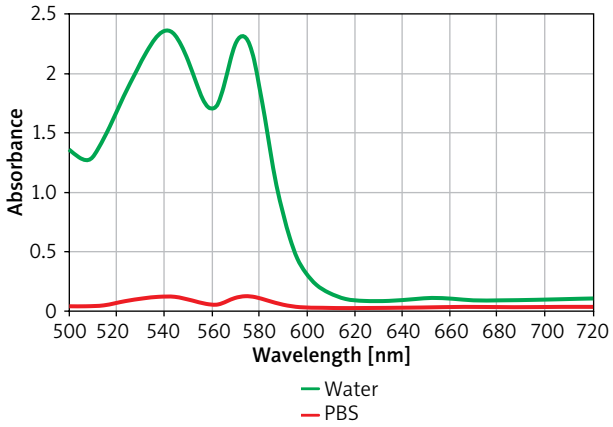

Figure 3. Different concentrations of UV (density range 50–400 μG/ml) – hemolysis test of nanomaterials

ment iron is in the human body, and iron ion can become a part of the normal iron content in the organism (such as ferritin, hemoglobin, transferrin and hemoglobin). For insoluble magnetic particles, the surface structure is more important than the chemical structure, so the surface and packaging of nanoparticles can be adjusted. In addition, the toxicity of ferric oxide nanoparticles is directly related to the concentration of oil required for diagnosis or treatment results. The active targeting strategy allows nanoparticles to concentrate on target organs, so the toxicity will appear to be very small.

Fe_3O should be further measured in the experiment 4@Au Blood compatibility of materials. First, one should take human blood, then wash the centrifuge (2000 rpm, 10 min), collect red blood cells with PBS 5 times, and then dilute 10 times of red blood cells. Then one should prepare Fe_3O_4@Au (50–400 μG/ml) nanoparticle suspension, and then 0.9 ml of Fe_3O_4@Au Mix with red blood cells diluted to 0.1 ml. After standing for 2 h, it should be centrifuged at 10000 rpm/min for 1 min, and then the value of supernatant should be measured.

As shown in Figure 3, PBS and PBS solutions containing different concentrations of Fe3O nanomaterials are non-hemolytic. The size of nanoparticles also affects their cycle time in organisms. Nanoparticles with a hydrodynamic diameter smaller than the glomerular porous size (about 10 nm) are rapidly excreted by the kidney in the form of urine, so their circulation time is relatively short. Nanoparticles larger than 100 nm are easily removed by macrophages. Therefore, if the nanoparticles are to have a long cycle time, the overall size of the nanoparticles should not be too small to prevent the rapid filtration of the kidney, and therefore should not be too large, which is increasingly taken over by macrophages.

Study population

Case selection

In this study 10 patients with locally uncontrolled recurrent head and neck squamous cell carcinoma admitted from August 2021 to February 2023 were selected.

Treatment

1) Inter-tissue implantation anesthesia: first, intramuscular injection of 50–100 mg of prednisolone, 10 mg of diazepam, and 5–25 ml of 2% lidocaine into the needle area (submaxillary area, sinus area, nasal cavity, submental area) for subcutaneous anesthesia.

2) Implantation method of the applicator: place the patient's lesion site (supine, lateral, seated) on the operating table or hospital bed, lay a sterile towel under local anesthesia, and comprehensively judge the scope of the primary lesion according to the CT, magnetic resonance imaging (MRI) and clinical physical examination palpation. Under the real-time guidance of B-ultrasound or CT, and with the assistance of 3D printing template, avoid important blood vessels, percutaneous puncture with a special radiotherapy needle to the edge of the tumor, and implant the cloth tube according to the Paris dosimetry system. The source pipes should be parallel and equidistant as far as possible, arranged in a square or equilateral triangle, and the distance between the source pipes should be 7–15 mm. The angle and depth of the insertion needle should follow the following four principles: the insertion needle should pass through the center of the tumor as far as possible; the insertion direction must be staggered from the internal carotid artery; the angle of insertion needle should be as small as possible; multi-needle insertion should be used as much as possible, especially for those with large tumors. The number of needles should be determined according to the size and scope of the tumor. The needle core should be inserted, and the depth of needle insertion should be measured by B-ultrasound or CT. After the needle core is stuck, it should be fixed with gauze and applied externally.

3) CT scanning localization: perform localization enhanced CT scanning in the supine position, with the scanning layer thickness of 2 mm, from the skull base to the lower edge of the clavicle. After scanning, observe whether the implantation position of the applicator meets the requirements. Then the qualiffed implanted CT images are transmitted to the Oncentra Masterplan planning system of the computer.

4) Develop three-dimensional afterloading treatment plan: CT enhancement or CT plain scan to determine the needle insertion and position, isocenter positioning film, orthogonal or variable angle positioning technology, determine the target area on the CT positioning film, select the source active residence site, conduct spatial reconstruction, and determine the treatment target area. Combined with the pre-radiotherapy, MRI and post-loading positioning CT images, the target area and sensitive organs were delineated on the Oncentra Masterplan system of the computer. GTV is a local recurrent lesion, and the sensitive organs mainly include skin, spinal cord, mandible, temporomandibular joint, etc. After the target area is delineated, the image is transmitted to the afterloading treatment planning system, the three-dimensional reconstruction of the applicator is carried

out, the source direction and length are determined, the GTV edge is used as the dose reference point, a single dose of 5–7 Gy is given, and then the dose optimization is carried out, so that the 100% dose curve can fully include GTV, and the radiation dose of the tissues outside the target area is minimized, and the brainstem, spinal cord, parotid gland, mandible, temporomandibular joint and other important organs are outside the 20–50% isodose curve.

5) Post-loading radiotherapy: use the 192Ir high-dose rate afterloading therapy machine of the Nuclear Power Company for treatment. The radiation source is 192Ir, with a diameter of 0.5 mm, a length of 3.5 mm, and a total dose of 10–24 Gy, 5–8 Gy/time, once/week. After the completion, one should immediately pull out the tube and record the depth of insertion into the submucosal applicator. The absolute value of the difference between the depth at the time of pin extraction and the depth at the time of pin insertion is counted as the drift length of the applicator. After extubating, patients were treated with pressure bandage to stop bleeding, and antibiotics were given during the post-loading treatment. The patients could eat orally without intravenous nutrition support.

Observation index and evaluation standard

The curative effect was evaluated according to Response Evaluation Criteria in Solid Tumors (RECIST) [18], and the degree of tissue and organ injury was observed according to the Toxicity criteria of the Radiation Therapy Oncology Group (RTOG) [19] as acute radiation injury grading standard.

Results

The mean age of the included patients was 38.5 ±10.7 years. Among them, there were 7 cases of moderately and poorly differentiated squamous cell carcinomas and 3 cases of highly differentiated squamous cell carcinomas. The diagnosis of recurrence and local uncontrollable disease was established through B-ultrasound, CT scans, and pathology. Following the administration of radiotherapy and chemotherapy (median radiotherapy dose of 70 Gy), 10 patients experienced uncontrolled recurrence and treatment failure. This comprised 4 cases of uncontrolled recurrence of primary lesions and 7 cases of uncontrolled recurrence in cervical lymph nodes (Table 1).

According to the Response Evaluation Criteria in Solid Tumors (RECIST) [18], CT scans were performed within 1–-6 months, with a subsequent 24-month follow-up. The results revealed complete response (CR) at 40% (4/10), partial response (PR) at 50% (5/10), no change (NC) at 10% (5/10), and progressive disease (PD) at 0 (Table 2). The overall effective rate, combining CR and PR, was 90% (9/10), with rates of 90% at 6 months, 80% at 12 months, 70% at 18 months, and 70% at 24 months. The overall survival rate at 24 months was 100%.

According to the RTOG, the incidence of grade I skin acute radiation injury was 70%, and the occurrence of grade II skin acute radiation injury was 10%. Furthermore, the frequency of grade I salivary gland acute radiation injury was 90%, and the rate of grade I hematological acute radiation injury was 20% (Table 3).

Discussion

The pathology of head and neck malignant tumors is mainly squamous cell carcinoma, so surgery or radiotherapy is usually selected for treatment. Its purpose is to improve the survival rate of patients and the control rate of tumors, minimize complications and reduce the rate of distant metastasis [20]. Uncontrolled or recurrent tumors in local areas are the main reasons that affect the overall survival rate of patients. How to improve the tumor control and survival rate of patients with recurrent head and neck squamous cell carcinoma after radiotherapy? It is a difficult problem for radiation oncologists to minimize the serious radiation damage caused by the second radiotherapy of adjacent sensitive organs, and to provide the opportunity for re-treatment after the local uncontrolled recurrence of head and neck squamous cell carcinoma invaded adjacent important organs [21]. In addition, although some good progress has been made in the comprehensive treatment based on radiotherapy and chemotherapy, the limitations and side effects of traditional external radiotherapy and intravenous chemotherapy have not changed. Therefore, it is still worthwhile to explore a more effective treatment method to minimize the damage to patients during the treatment process while treating patients.

Short-range radiotherapy plays an important role in the treatment of head and neck tumors. Because the radiation source is directly irradiated in the tumor target

Table 1. General characteristics of patients included in the study

Variables		Result
Gender	Male	9
	Female	1
Age	Mean	38.5±10.7
Disease type	Nasopharyngeal carcinoma	4
	Carcinoma of maxillary sinus	3
	Laryngeal carcinoma	2
	Carcinoma of nasal cavity	1
Degree of differentiation	Middle and low differentiation	7
	Highly differentiated	3
Uncontrolled recurrence	Primary focus	4
	Cervical lymph nodes	7

Table 2. Response evaluation of patients undergoing non-coplanar template brachytherapy (%)

Total number of patients Curative effect	CR	PR	NC	PD	Total efficiency CR + PR
10	4 (40)	5 (50)	1 (10)	0 (0)	9 (90)

Table 3. Prevalence of acute radiation injury rate of organs and tissues (%)

Organ tissue damage	*N*	Level 0	Level 1	Level 2	Level 3	Level 4
Skin	10	2 (20)	7 (70)	1 (10.0)	0 (0)	0 (0)
Salivary gland	10	1 (10)	9 (90)	0 (0)	0 (0)	0 (0)
Hematology	10	8 (20)	2 (20)	0 (0)	0 (0)	0 (0)

area, the treatment area can be irradiated with a high dose, and the dose outside the reference point decreases rapidly, which can effectively protect the surrounding important organs [22]. Due to the complex anatomical structure of the head and neck tumors, dense blood vessels and nerves, and the limited access of the insertion needle, it is difficult to arrange according to the Paris system, affecting the treatment effect and high risk. It is difficult to implant with bare hands. Due to the influence of complex anatomical factors, there is great uncertainty in the simple B-ultrasound or CT image-guided implant operation, and the implant accuracy is highly dependent on clinical experience. In recent years, with the progress of 3D printing technology, the 3D printing single non-coplanar template (called 3D printing template) produced by computer-aided rapid prototyping is very fast, which also improves its accuracy and safety. The 3D printing coplanar template derived from it has been widely used in radioactive 125I particle implantation therapy [23]. The application of 3D printing coplanar template has greatly improved the stability of the puncture needle and made the puncture more accurate. In addition, it can ensure that multiple puncture needles are parallel to each other, greatly reducing the difficulty of puncture, shortening the operation time, and thus reducing the discomfort of patients due to long-term operation. The 3D core of CT images is equipped with a close-range planning system. The insertion needles can be arranged arbitrarily according to the shape of CTV, and the intersection and dislocation of each other do not affect the optimization of the plan. By reconstructing the 3D position of each needle, one can define the location and reception of GTV, CTV and organs at risk, and use the reverse treatment planning system to optimize the residence time of each point, so as to adjust the dose of each point, so that the combined dose is highly conformable to the treatment target area. It makes it possible for the tumor area to be precisely irradiated by high dose. Therefore, Sharma *et al.* believe that the intensity-modulated radiotherapy guided by inter-tissue implantation has obvious dosimetric advantages compared with traditional afterloading radiotherapy.

As early as in the 1950s and 1960s, it was reported in the literature that the treatment of oral and oropharyngeal cancer with radium needle implantation could achieve the same effect as surgery, but the staff was abandoned due to the high dose of radium pollution. Thiel *et al.* reported 55 cases of head and neck implant radiotherapy, 10 Gy times, once a day, for 2 to 3 days. As a result, 4 cases had mandibular necrosis and needed surgical treatment. They suggested reducing the dose of each irradiation. In the past decade, the wide application of a high dose rate 192Ir stepping source afterloading machine and computer treatment planning system has led to the resurgence of intra-tissue irradiation therapy. External irradiation alone cannot achieve satisfactory results for head and neck squamous cell carcinoma that has not been locally controlled in the past. Increasing the dose of external irradiation can easily cause damage to surrounding normal tissues, such as jaw bone necrosis, radiation osteomyelitis, etc. However, the invention of 3D printing technology provides new ideas for radiotherapy. Michaels *et al.* used 3D printing technology for the first time in proton therapy of patients with oropharyngeal cancer to make skin compensation membrane and proton range regulator for superficial lesions. Compared with traditional solutions, the solution using 3D printing technology can reduce the average probability of dry mouth by 3% and the symptoms of dysphagia by 2.7%. Wochnik *et al.* used 3D printing technology to make personalized range compensator and field compensator in proton therapy of children's brain tumors, and the results showed that the air gap could be further reduced, thus reducing proton scattering. For organs close to the radiation field and other centers, such as thyroid, the scattering dose is very low, which does not lead to the increase of secondary radiation. Inspired by the above, we used B-ultrasound or CT-guided 3D printing to personalize the non-coplanar template short-distance interstitial implantation brachytherapy to explore a new treatment mode for locally uncontrolled recurrent head and neck squamous cell carcinoma.

In a study by Liu *et al.* [24], pre-plan and post-plan dosimetric parameters of 3D-PNCT-assisted CT-guided RISI in inguinal lymph node metastatic patients were analyzed. A total of 15 patients were evaluated, with 60% achieving a CR, 27% showing a PR, and 13% demonstrating stable disease (SD). The local control (LC) rates at 1- and 3-year intervals were 92%, and the progression-free

survival (PFS) rates at 1- and 3-year intervals were 79% and 32%, respectively, with a median PFS of 24 months. The overall survival (OS) rates at 1- and 3-year intervals were 79% and 37%, respectively, with a median OS of 29 months. These results were similar to our study findings.

Another study by Wang *et al.* [25] investigated the feasibility of CT-guided radioactive 125I seed (RIS) implantation assisted with three-dimensional printing non-coplanar template (3D-PNCT) in locally recurrent rectal cancer (LRRC) patients who previously received surgery or external beam radiotherapy (EBRT). Three months following the seed implantation, the rates of CR, PR, SD, and progressive disease (PD) were 18.2% (12/66), 66.7% (44/66), 10.6% (7/66), and 4.5% (3/66), respectively.

Traditional clinical contrast agents have some side effects, among which the time of circulation of small molecule drugs is too short and easy to be metabolized. Therefore, in the gradual evolution, most of the contrast agents used in clinical use at this stage are CT, MRI or photocoagulation inhibiting single contrast agents [26, 27]. Different detection methods need to inject different contrast agents, which has special complications in diagnosis. Therefore, it increases the psychological burden of patients. Ionic and non-ionic types are the main components of CT technology [27]. The advantage of the ionic contrast agent is that it is fast to contrast. In order to achieve the best development effect, a larger dose of injection is required. This causes damage to the blood-brain barrier, and also causes vasodilation, myocardial injury and local fever interference. Non-ionic contrast agent improves the physical and chemical properties related to the ionic form. After the non-ionic contrast agent enters the body, it is mainly manifested as the concentration of iodine. The flow rate of the non-ionic contrast agent is slow, and the circulation time is long, which helps to obtain images [28]. In order to provide reliable data support for clinical practice, non-ionic contrast agents are different from previous ionic contrast agents, but there are also some side effects, the main side effect of which is high injection density. The osmotic pressure of the ionic contrast agent is higher than that of the non-ionic form, which is much higher than that of body blood, so it causes adverse reactions. Because nanomaterials have a certain particle size, good compatibility can be achieved through surface modification, and the time of internal circulation can be prolonged. Therefore, using nanomaterials as contrast agents is a research direction at this stage.

Conclusions

The results of this study show that B-ultrasound or CT-guided 3D printing individualized non-coplanar template brachytherapy can safely and effectively treat uncontrolled recurrent head and neck squamous cell carcinoma, especially for cervical lymph node recurrence and metastasis. B-ultrasound or CT-guided 3D printing assisted individualized non-coplanar template brachytherapy can better protect organ function, with less side effects and fewer complications. It is one of the best methods to treat locally uncontrolled recurrent head and neck squamous cell carcinoma, and is worthy of clinical promotion.

Acknowledgments

Health Industry Research Project in Gansu Province (No. GSWSKY2022-23).

Conflict of interest

The authors declare no conflict of interest.

References

1. Citrin DE. Recent developments in radiotherapy. N Engl J Med 2017; 377: 1065-75.
2. Chandra RA, Keane FK, Voncken FE, Thomas CR. Contemporary radiotherapy: present and future. Lancet 2021; 398: 171-84.
3. Stein AP, Saha S, Kraninger JL, et al. Prevalence of human papillomavirus in oropharyngeal cancer: a systematic review. Cancer J 2015; 21: 138-46.
4. Isayeva T, Li Y, Maswahu D, Brandwein-Gensler M. Human papillomavirus in non-oropharyngeal head and neck cancers: a systematic literature review. Head Neck Pathol 2012; 6 Suppl 1: 104-20.
5. Michaud DS, Langevin SM, Eliot M, et al. High risk HPV types and head and neck cancer. Int J Cancer 2014; 135: 1653-61.
6. Johnson DE, Burtness B, Leemans CR, et al. Head and neck squamous cell carcinoma. Nat Rev Dis Primers 2020; 6: 92.
7. Schwarz R, Bruland O, Cassoni A, et al. The role of radiotherapy in oseosarcoma. Cancer Treat Res 2009; 152: 147-64.
8. Barazzuol L, Coppes RP, van Luijk P. Prevention and treatment of radiotherapy-induced side effects. Mol Oncol 2020; 14: 1538-54.
9. Löbrich M, Kiefer J. Assessing the likelihood of severe side effects in radiotherapy. Int J Cancer 2006; 118: 2652-6.
10. Kwan W, Wilson D, Moravan V. Radiotherapy for locally advanced basal cell and squamous cell carcinomas of the skin. Int J Radiation Oncol Biol Phys 2004; 60: 406-11.
11. Whittig L, Allardice W. X-ray diffraction techniques. Methods of soil analysis: part 1. Phys Mineral Methods 1986; 5: 331-62.
12. Süncksen M, Bendig H, Teistler M, et al. editors. Gamification and virtual reality for teaching mobile x-ray imaging. 2018 IEEE 6th international conference on serious games and applications for health (SeGAH); 2018: IEEE.
13. Ginat DT, Gupta R. Advances in computed tomography imaging technology. Ann Rev Biomed Engineering 2014; 16: 431-53.
14. Kapila S, Conley R, Harrell Jr W. The current status of cone beam computed tomography imaging in orthodontics. Dentomaxillofac Radiol 2011; 40: 24-34.
15. Keall P. 4-dimensional computed tomography imaging and treatment planning. Semin Radiat Oncol 2004; 14: 81-90.

16. Shah AP, Langen KM, Ruchala KJ, et al. Patient dose from megavoltage computed tomography imaging. Int J Radiat Oncol Biol Phys 2008; 70: 1579-87.
17. Engelke K, Museyko O, Wang L, Laredo JD. Quantitative analysis of skeletal muscle by computed tomography imaging – state of the art. J Orthop Transl 2018; 15: 91-103.
18. Wolchok JD, Hoos A, O'Day S, et al. Guidelines for the evaluation of immune therapy activity in solid tumors: immune-related response criteria. Clin Cancer Res 2009; 15: 7412-20.
19. Cox JD, Stetz J, Pajak TF. Toxicity criteria of the Radiation Therapy Oncology Group (RTOG) and the European Organization for Research and Treatment of Cancer (EORTC). Int J Radiat Oncol Biol Phys 1995; 31: 1341-6.
20. Cunningham MJ, Myers EN, Bluestone CD. Malignant tumors of the head and neck in children a twenty-year review. Int J Pediatr Otorhinolaryngol 1987; 13: 279-92.
21. García J, López M, López L, et al. Validation of the pathological classification of lymph node metastasis for head and neck tumors according to the 8th edition of the TNM Classification of Malignant Tumors. Oral Oncol 2017; 70: 29-33.
22. Berbeco RI, Ngwa W, Makrigiorgos GM. Localized dose enhancement to tumor blood vessel endothelial cells via megavoltage X-rays and targeted gold nanoparticles: new potential for external beam radiotherapy. Int J Radiat Oncol Biol Phys 2011; 81: 270-6.
23. Shahrubudin N, Lee TC, Ramlan R. An overview on 3D printing technology: technological, materials, and applications. Proced Manufacturing 2019; 35: 1286-96.
24. Liu Y, Shen Z, Qu A, et al. A comparative study of dosimetric parameters of 3D-printed non-coplanar template-assisted CT-guided iodine-125 seed implantation brachytherapy in patients with inguinal lymph node metastatic carcinomas. J Contemp Brachyther 2022; 14: 452-61.
25. Wang L, Wang H, Jiang Y, et al. The efficacy and dosimetry analysis of CT-guided 125I seed implantation assisted with 3D-printing non-co-planar template in locally recurrent rectal cancer. Radiat Oncol 2020; 15: 179.
26. Hasebroock KM, Serkova NJ. Toxicity of MRI and CT contrast agents. Exp Opin Drug Metabol Toxicol 2009; 5: 403-16.
27. Caschera L, Lazzara A, Piergallini L, et al. Contrast agents in diagnostic imaging: present and future. Pharmacol Res 2016; 110: 65-75.
28. Wolf GL, Arenson RL, Cross A. A prospective trial of ionic vs nonionic contrast agents in routine clinical practice: comparison of adverse effects. Am J Roentgenol 1989; 152: 939-44.